

Statistical Test-Based Practical Methods for Detection and Quantification of Stiction in Control Valves

Seshu K. Damarla, Xi Sun, Fangwei Xu, Ashish Shah, and Biao Huang*



Cite This: *Ind. Eng. Chem. Res.* 2023, 62, 4410–4421



Read Online

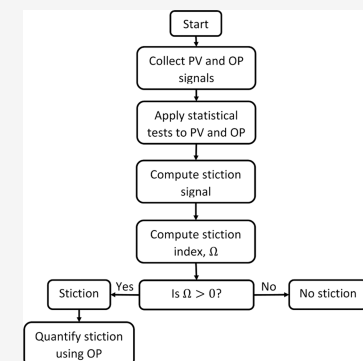
ACCESS |

Metrics & More

Article Recommendations

Supporting Information

ABSTRACT: Control valve, affected by stiction, causes closed-loop signals to experience oscillations, which ultimately leads to a decrease in product quality, reduced plant throughput, and increased environmental footprint. Therefore, it is indispensable to detect and quantify stiction in control valves. To accomplish this objective, in the present work, four noninvasive practical and simple methods are developed with the help of statistical tests such as *F*-test, *t*-test (Student's *t*-test), modified Hotelling T^2 -test, and reverse arrangement test (RAT). The developed methods are applied to benchmark control loops espoused from chemical, paper, and mining industries. The results of the proposed methods are compared with that of existing methods found in the literature. It is found that the *t*-test-based method, the modified Hotelling T^2 -test-based method, and the RAT-based method demonstrate equally good or better performance than the existing methods, while the *F*-test-based method outperforms some of the existing methods. In addition to detecting stiction, the proposed methods can quantify stiction to timely notify panel operators of stiction severity and assist plant maintenance engineers to arrange plant shutdowns well ahead in time. The proposed methods are applicable to all types of control loops except level loops.



1. INTRODUCTION

Process industries encounter, on a regular basis, challenging operational issues instigated by poorly performing control loops.^{1,2} Owing to this fact, academia and industry witnessed, in the past two decades, expeditious progress in research activities aimed at monitoring and assessing the performance of the control loops. Oscillations can often be the symptoms of the control loops behaving badly and may have ramifications such as reduced product quality, amplified usage of plant utilities, and hastened equipment aging, all of which will eventually result in interrupted plant operations. There can be multiple causes triggering oscillations in the control loops. The most common root causes are aggressive controller tuning, process upsets (external disturbances), sensor faults, and control valve faults (deadband, hysteresis, stiction, etc.). According to the industrial survey conducted by Bialkowski,³ valve faults are actually the source of oscillations in nearly one-third of control loops in Canadian paper mills. Stiction occurs more regularly and is more detrimental than the rest of the valve faults. It induces controller output (OP) and process variable (PV) to exhibit cycling behavior. Therefore, it is of the utmost importance to detect and quantify stiction in control valves. The identification of sticky control valves is easy if the measurements of valve stem position are available. However, in practice, those measurements are seldom obtainable. Thus, detecting the presence of stiction is a challenging problem. This research problem draws a great deal of attention from academia and industry. Numerous methods have been reported in the literature, which generally fall into invasive and noninvasive categories. Albeit the invasive methods offer

irrefutable results, their application interferes with the routine operation of the plant, requires field tests (valve travel test or bump test), and they are difficult to implement. On the contrary, noninvasive methods do not disturb the running plant and are easier to deploy in industrial settings. The existing noninvasive methods depend on limit cycles, waveform shapes, nonlinearity detection, multivariate statistical techniques, machine learning or deep learning algorithms, and optimization methods.^{4–10}

Statistical tests offer means to make quantitative decisions with regard to a process. The purpose of employing the statistical tests is to determine if there is adequate evidence to reject a hypothesis (for instance, given two data sets having the same variance) regarding the process. The available statistical tests can be categorized into parametric and nonparametric statistical tests. The parametric (or parameter bound) statistical tests, such as *F*-test, *t*-test, Hotelling T^2 -test, variance ratio test, and so on, entail calculation of one or more statistical properties (mean, standard deviation, etc.) of process data being examined.^{11–14} Whereas the nonparametric statistical test, like the reverse arrangement test, sidesteps parameter calculation of any kind and makes decisions by comparing

Received: October 5, 2022

Revised: February 3, 2023

Accepted: February 22, 2023

Published: March 1, 2023



observations (or data points) against each other.¹⁵ The traditional applications of statistical tests include equipment-agging test, determining equipment dynamic damage, and machines comparison with respect to product quality, to name a few.¹¹ Besides, the statistical tests have an interesting use in process systems engineering, i.e., real-time identification of steady states in chemical process data.^{14,16,17} Such steady-state detection is the basis for process data reconciliation, process modeling, online optimization, and process performance assessment. Since their advent, statistical tests have been widely utilized in different technical fields, but their application in stiction detection is new. It is believed that methods making use of the statistical tests can provide a more accurate diagnosis for the oscillating control loops. The contribution of the present work lies in bringing forth four automatic stiction detection and quantification methods based on the *F*-test, the *t*-test, the modified Hotelling *T*²-test, and the reverse arrangement test. The remaining part of the paper is organized as follows. Section 2 introduces the research problem of control valve stiction. In Section 3, the theory of the proposed methods is provided. Section 4 presents the application of the proposed methods to industrial control loops. Section 5 offers conclusions drawn from the present study.

2. CONTROL VALVE STICKTION

Figure 1 illustrates the behavior of a sticky control valve. Because of the presence of stiction, OP has a nonlinear relation

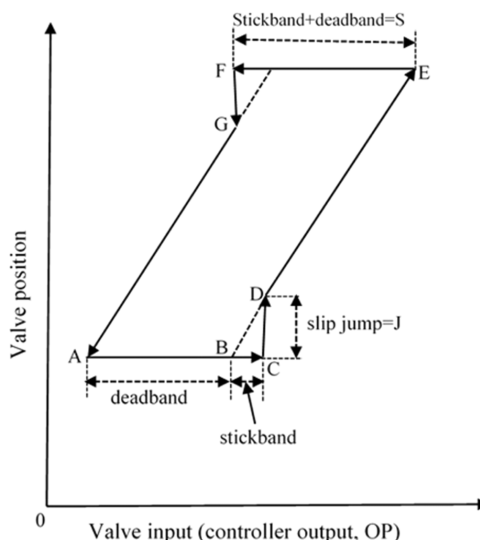


Figure 1. Relation between OP and valve position of a sticky control valve.¹⁸ In the figure, S is called the stiction band.

with valve stem position instead of a linear relation as in the case with a healthy valve. The closed-loop signals of the flow control loop, adopted from an international stiction database (ISDB) created by Jelali and Huang,⁴ with a sticky valve, are shown in Figure 2. The representative curve displayed in Figure 1 is shaped by deadband, stickband, slip-jump, and moving phase. During stiction, the valve stem stays at a constant value while OP is moving from point A–C. Owing to this, process input does not change, causing process variable (PV) to remain constant or vary slowly. This steady-state phase in PV lasts as long as the valve stem does not budge. Therefore, an offset is created between PV and setpoint (SP), which forces the controller to vary OP. When a cumulative

change in OP is adequate to push the valve, the valve is released from stiction and abruptly jumps from point C to point D, which is termed the slip-jump. From point D onward, the valve stem position keeps altering without pause (moving phase) so that both OP and PV change and are in nonsteady state. When the valve stem is in motion, PV in Figure 2 keeps varying, and this state is called the transient (or nonsteady) state. The transient state commences every time the valve overcomes stiction. When PV deviates from SP, the controller changes OP in an effort to bring PV back to SP. When OP begins to decrease at point E, the valve is blocked a second time, and as a result, PV enters a steady state. For a given time period, the valve may stick several times; consequently, PV can have numerous similar or dissimilar steady states (or pseudo-steady states because of noise), depending upon how SP changes. Figure 3 portrays the oscillating PV and OP of a concentration control loop, taken from ISDB, having a healthy valve (nonsticky valve). Since the oscillations in this control loop are induced by a non-stiction condition (inappropriate controller tuning) and the valve is free of stiction, PV and OP continuously vary, and there are no steady states in PV. The above discussion brings to light important points that when the valve stem does not move, PV stays unchanged (i.e., PV is in the steady state), and OP keeps varying (OP is in the transient state). If the valve stem position is changing, both PV and OP vary (in the same direction or the opposite direction), i.e., both PV and OP are in the transient state.

3. PROPOSED METHODS

As explained in the foregoing section, sticky control valves in industrial control loops can be detected by identifying steady state and nonsteady (transient) state periods in PV and OP signals, respectively. Aligned with this idea, the present work brings forward four noninvasive methods relying on statistical tests. As Methods 1, 2, and 3 function in a similar fashion, a common flowchart displayed in Figure 4 is used to spell out the different steps involved in them. Figure 5 explains the stiction detection process for Method 4.

3.1. Method 1. The building block of Method 1 is the *F*-test that is used to check if two consecutive data windows X_i and X_j have the same variance.¹¹ The *F*-test is calculated as given in eq 1.

$$F = \frac{s_i^2}{s_j^2} \quad (1)$$

where s_i^2 and s_j^2 are the variances of X_i and X_j , respectively.

The critical *F*-value (F_α) is derived using numerator degrees of freedom ($f_1 = n_i - 1$, where n_i is the number of data points in X_i), denominator degrees of freedom ($f_2 = n_j - 1$, where n_j is the number of data points in X_j), and significance level α , from *F*-distribution (or Fisher–Snedecor distribution). The critical *F*-value is used to corroborate the hypotheses defined below.

Null hypothesis $H_0: s_i^2 = s_j^2$

Alternative hypothesis $H_1: s_i^2 \neq s_j^2$

If *F*-value is less than the critical *F*-value at the significance level α , the alternative hypothesis is rejected, which means X_i and X_j are in a steady state. Otherwise, the null hypothesis is rejected so that X_i and X_j are not in the steady state (one of them is in the transient state, and the other one is in the steady state, or both of them are in the transient state).

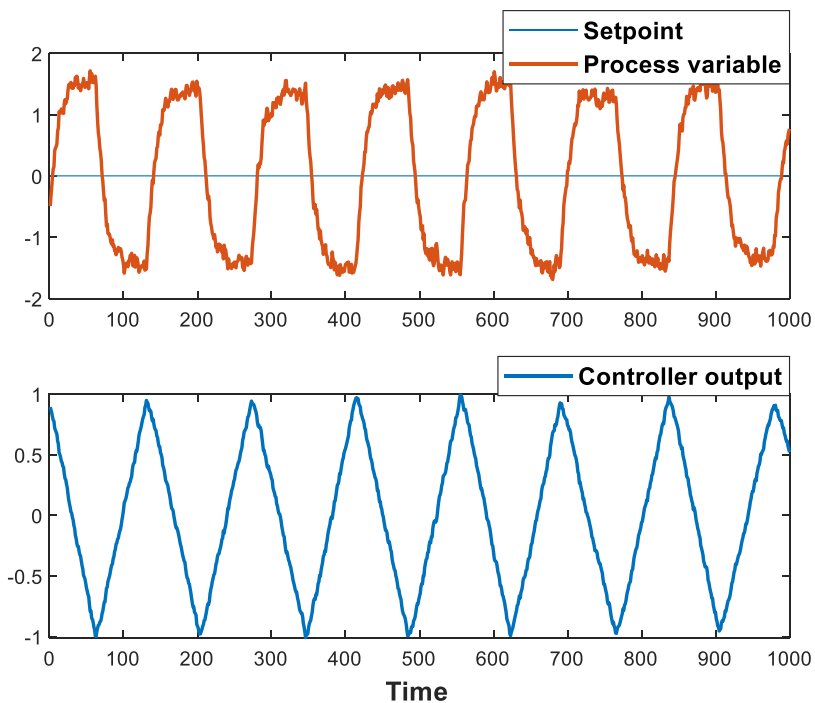


Figure 2. Flow control loop with a sticky valve.

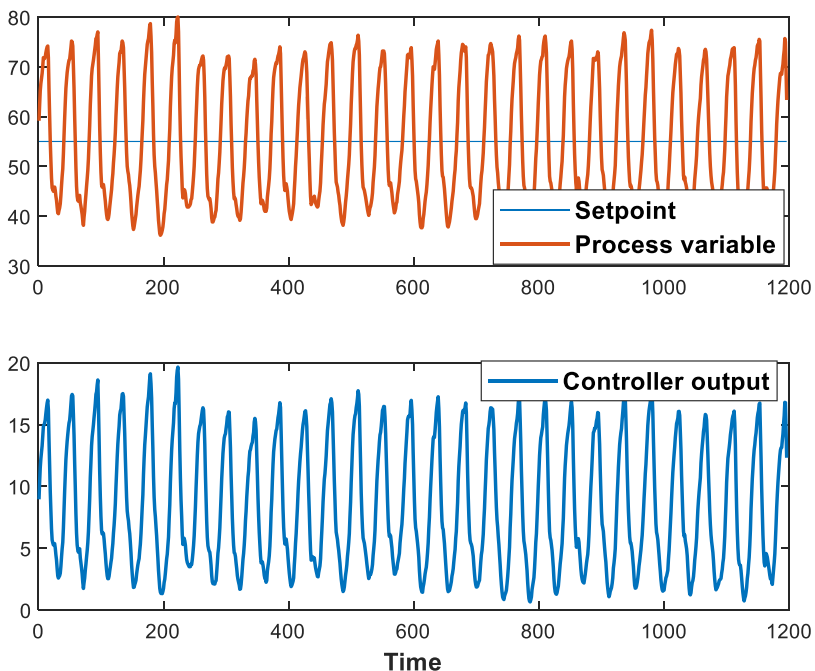


Figure 3. Concentration control loop with a healthy valve.

The process of detecting stiction with the help of Method 1 is shown in **Figure 4** and delineated below.

Step 1. Select optimal values for the window size w_s and significance level α . Calculate $N = \text{length}(PV)/w_s$. If N is a noninteger, it is rounded to the nearest integer.

Step 2. Consider raw PV and OP. The determination of steady or transient-state periods is independently carried out for PV and OP.

Step 3. The F-test is applied to the first two data windows NP_1 and NP_2 (size of each data window is w_s) of PV, and F^{PV} is computed as per eq 1.

Step 4. F^{OP} is calculated using the first two data windows NQ_1 and NQ_2 of OP.

Step 5. If $F^{PV} < F_\alpha^{PV}$ (steady state) and $F^{OP} \geq F_\alpha^{OP}$ (transient state), the control valve is sticky in the first and second data windows, so $S(1) = 1$ and $S(2) = 1$ (where S is the stiction signal). If not, the control valve continuously moves; therefore, $S(1) = 0$ and $S(2) = 0$.

Step 6. The second and third data windows of PV and OP are considered. F^{PV} and F^{OP} are calculated. The condition given in Step 5 is verified, and accordingly, one or zero is

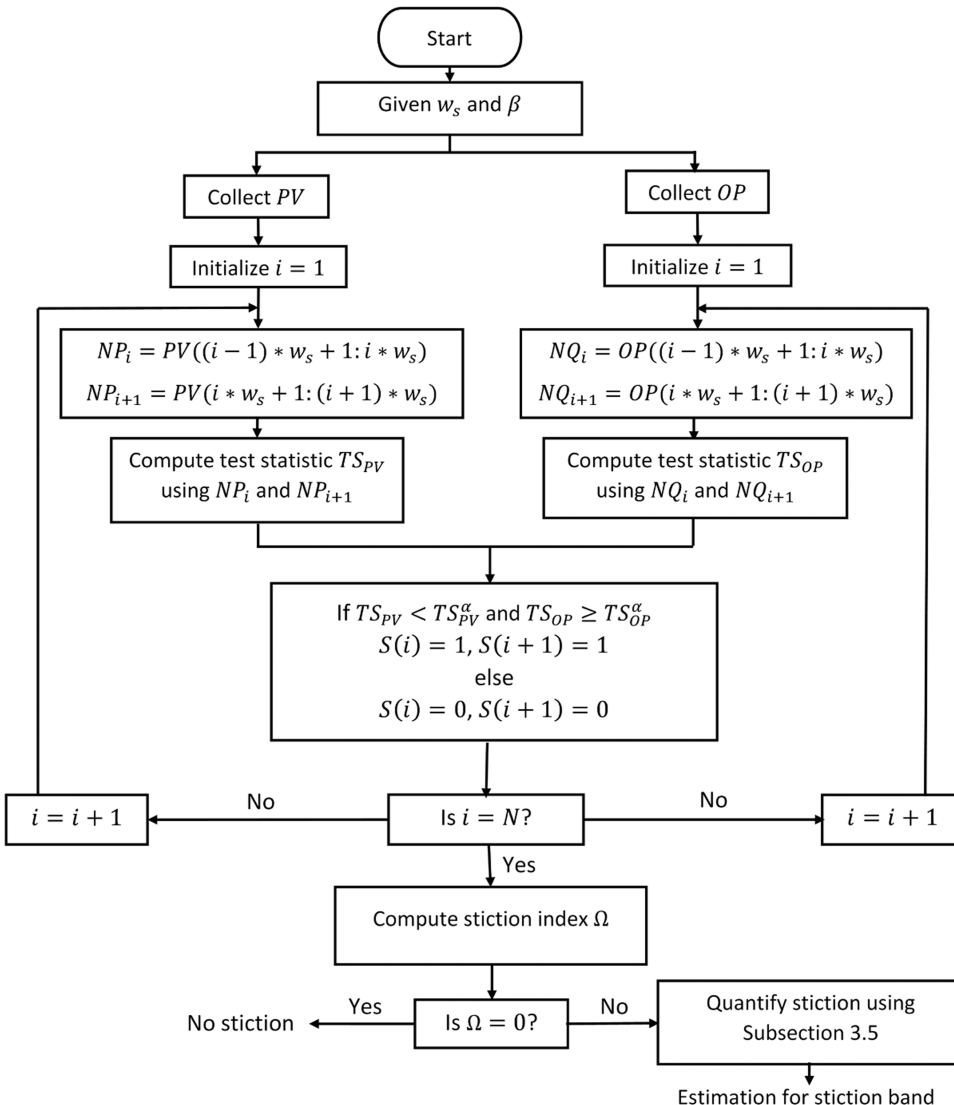


Figure 4. Common stiction detection procedure for Methods 1, 2, and 3. Here, TS denotes a test statistic that can be *t*-test value t_p , *F*-value, and modified T^2 -test value $T_{pf,B}^2$. TS^α is the corresponding critical value obtained at α . N is the total number of data windows of PV or OP.

assigned to $S(2)$ and $S(3)$. This procedure is repeated for the remaining data windows of PV and OP.

Step 7. Stiction index Ω is computed using the following equation

$$\Omega = \frac{\sum_{i=1}^N S(i)}{N} \quad (2)$$

A nonzero value of Ω confirms the presence of stiction. If $\Omega = 0$, the oscillations in the given control loop are caused by a non-stiction condition.

Step 8. If stiction is detected in Step 7, the stiction quantification method provided in Section 3.5 is used to quantify the degree of stiction.

3.2. Method 2. Method 2 is based on the *t*-test or Student's *t*-test, which is employed to verify whether the mean values (μ_i and μ_j) of X_i and X_j differ significantly.¹¹ The two-sample *t*-test employs mean and dispersion (standard deviation) to reject null or alternative hypothesis defined as follows.

Null hypothesis H_0 : μ_i and μ_j are equal.

Alternative hypothesis H_1 : μ_i and μ_j are not equal.

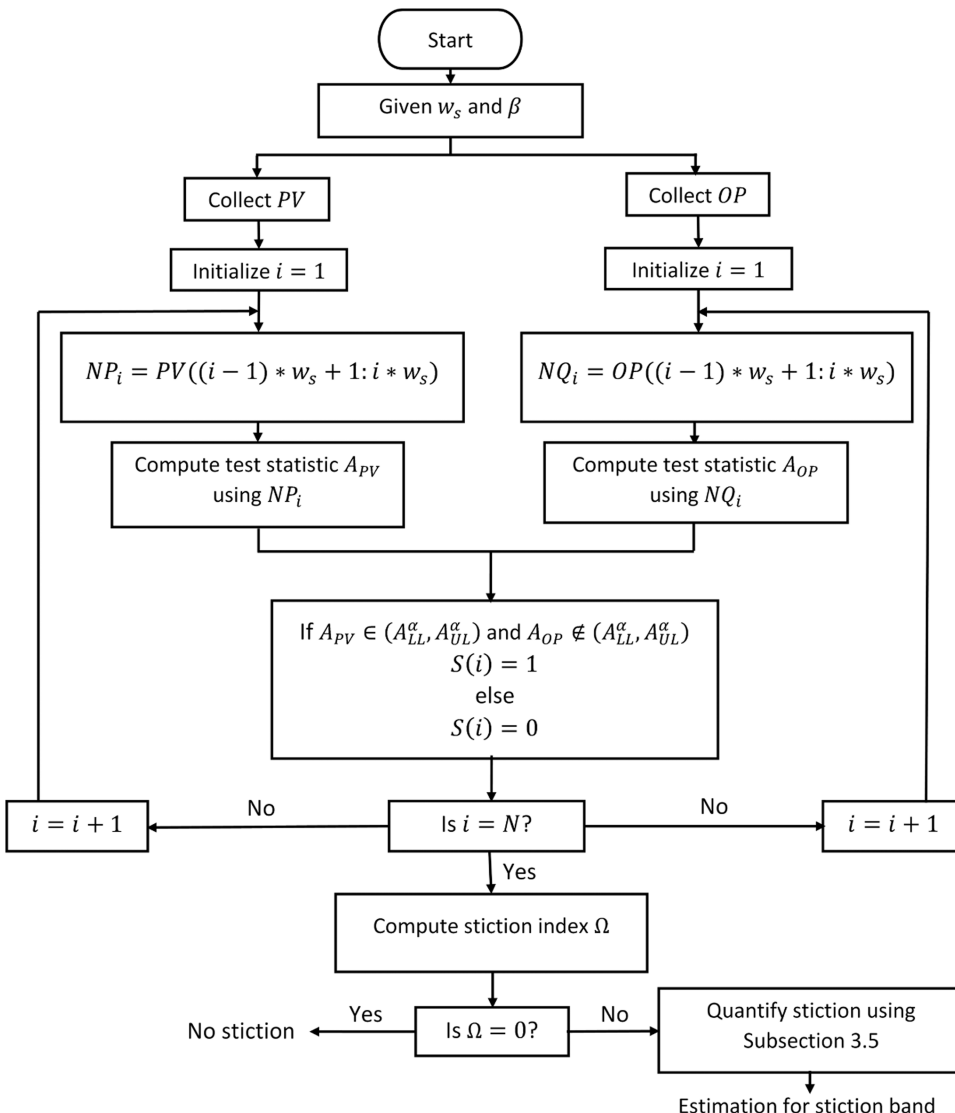
The *t*-value (or test value t_p) is defined as follows

$$t_p = \frac{|\mu_i - \mu_j|}{s_d \sqrt{\frac{1}{n_i} + \frac{1}{n_j}}} \quad (3)$$

$$\text{where } s_d = \sqrt{\frac{(n_i - 1)s_i^2 + (n_j - 1)s_j^2}{n_i + n_j - 2}}.$$

In eq 3, s_i and s_j are the standard deviations of X_i and X_j respectively. The denominator in the expression for s_d is the degree of freedom f . Once the t_p -value is computed, it is compared against the critical t_p -value ($t_{p,\alpha}$) obtained from *t*-distribution. If the t_p -value, at the given significance level α , is less than $t_{p,\alpha}$ the alternative hypothesis is rejected, i.e., the data windows are in a steady state. Otherwise, the null hypothesis is rejected; hence, the data windows are not in a steady state.

The second method works exactly the same as the first method to ascertain the presence of stiction in control valves. Since the second method uses the *t*-test, w_s and α have different optimal values. In Steps 3 and 4 of the stiction detection procedure for Method 1, the t_p -values are computed for PV and OP instead of the *F*-values. In Step 5, the computed

**Figure 5.** Stiction detection procedure for Method 4.

t_p -values are compared with the corresponding $t_{p,\alpha}$. The rest of the process remains the same.

3.3. Method 3. By applying the modified Hotelling T^2 -test defined in eq 4, Method 3 looks over if X_i and X_j have the same mean.^{12,13}

$$T_{pf_B}^2 = 0.5wsd'S^{-1}d \quad (4)$$

where $d = \mu_i - \mu_j$, $S = (A_i + A_j)/(2n)$, $A_i = \sum_{k=1s}^w (X_{ik} - \mu_i)(X_{ik} - \mu_i)'$, $A_j = \sum_{k=1s}^w (X_{jk} - \mu_j)(X_{jk} - \mu_j)'$, and $n = \text{length}(X_i) - 1$.

Critical value ($T_{pf_B,\alpha}^2$) for the test statistic in eq 4 is obtained from eq 5.

$$T_{pf_B,\alpha}^2 = \frac{pf_B F_{pf_B-p+1}^\alpha}{f_B - p + 1} \quad (5)$$

where $f_B = n/A$, $A = \left(\frac{d's^{-1}Ss^{-1}d}{2d's^{-1}d} \right)^2 + \left(\frac{d's^{-1}Ss^{-1}d}{2d's^{-1}d} \right)^2$, $S_i = A_i/n$, $S_j = A_j/n$, $S = (S_i + S_j)/2$, $p = 1$, and $F_{pf_B-p+1}^\alpha$ is the F -value, obtained at the significance level α , from the F -distribution, with the numerator degree of freedom p and the denominator degree of freedom $f_B - p + 1$.

In eq 5, p denotes the number of variables in X_i or X_j . In the present work, the closed-loop signals PV and OP are separately analyzed, so $p = 1$. The same flowchart shown in Figure 4 is applicable to the third method. As each of the data windows contains different data points, $T_{pf_B,\alpha}^2$ is different for different data windows.

3.4. Method 4. Method 4 hinges on the reverse arrangement test to find out steady- and nonsteady-state periods in PV and OP, respectively.¹⁵ It is not required for the reverse arrangement test to compute any statistical property (mean, standard deviation, etc.) of the data being analyzed. Let us consider a sequence of M observations: $x_1, x_2, x_3, x_4, \dots, x_{M-1}, x_M$. Now, count the number of times that $x_1 > x_j$ for $1 < j$. This inequality is called a reverse arrangement (A_1). The process is repeated for the remaining observations in the sequence: $x_2, x_3, x_4, \dots, x_{M-1}, x_M$. The total number of reverse arrangements is denoted by A .

$$A = \sum_{i=1}^{M-1} \left(\sum_{j=i+1}^M h_{ij} \right) \quad (6)$$

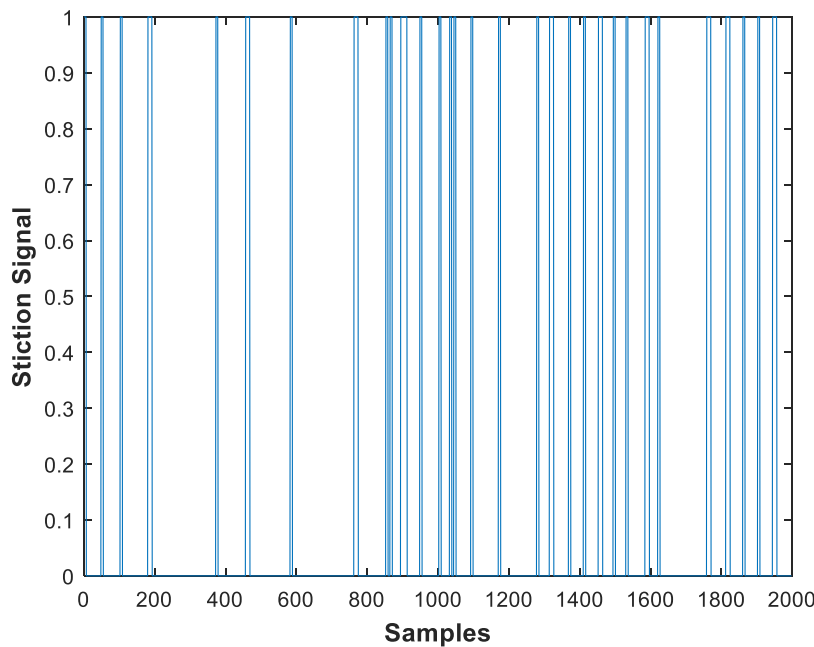


Figure 6. Stiction signal.

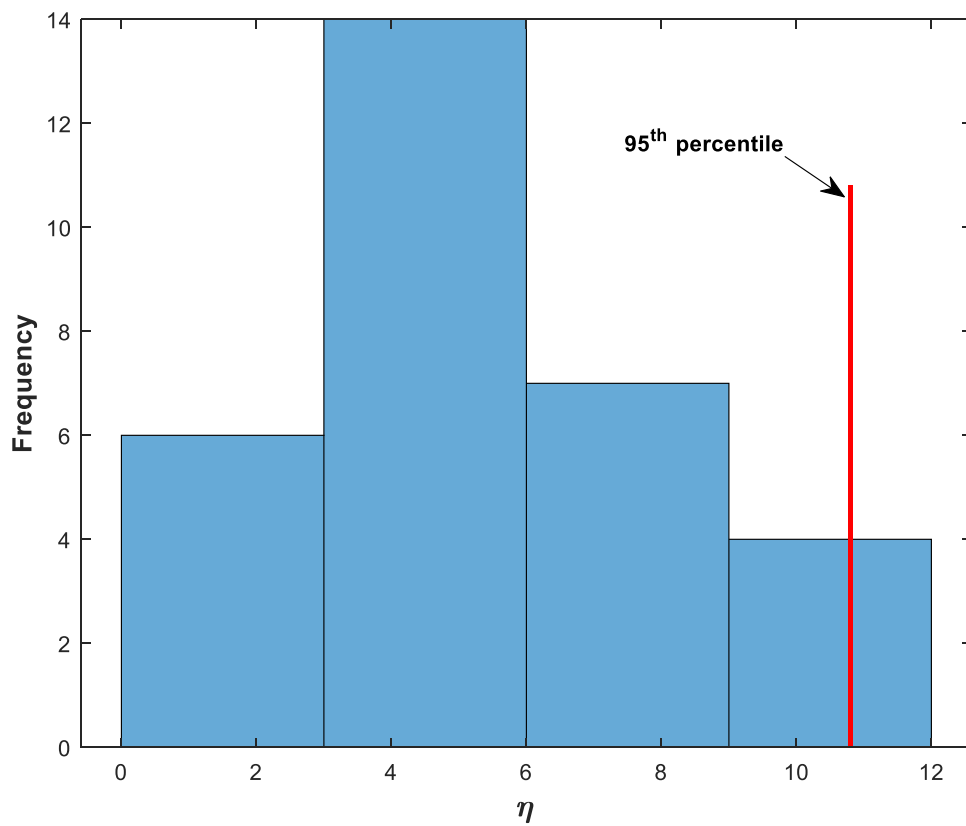


Figure 7. Distribution of η .

$$\text{where } h_{ij} = \begin{cases} 1 & \text{if } x_i > x_j \\ 0 & \text{otherwise} \end{cases}$$

The upper (A_{UL}^α) and lower limit (A_{LL}^α) for A can be computed using eqs 7 and 8, respectively.

$$A_{UL}^\alpha = z_\alpha \times \sigma_A + \mu_A - 0.5 \quad (7)$$

$$A_{LL}^\alpha = \mu_A - z_\alpha \times \sigma_A + 0.5 \quad (8)$$

where $\mu_A = \frac{M(M-1)}{4}$, $\sigma_A = \sqrt{\frac{2M^3 + 3M^2 - 5M}{72}}$, α is the significance level, and z_α is the area under the normal distribution curve at $(1 - \alpha)\%$ confidence interval.

If $A_{LL}^\alpha < A < A_{UL}^\alpha$, null hypothesis (the observations in the above sequence are in stationary or steady-state phase) is true. Otherwise, the alternative hypothesis (the observations are in nonstationary or transient phase) is true.

The way in which Method 4 detects sticky control valves is quite analogous to Methods 1, 2, and 3. Method 4 functions in accordance with the flowchart displayed in **Figure 5**.

Step 1: Optimal values for w_s and α are chosen. Given PV and OP signals are divided into N separate data windows, respectively.

Step 2: Like the above three methods, this method too can work with raw PV and OP. Hence, PV and OP do not need to be smoothed or denoised.

Step 3: The first data window of PV is selected: $NP_1 = PV(1:w_s)$. The reverse arrangement test is applied to NP_1 , and A_{PV} is calculated using **eq 6**.

Step 4: The first data window of OP is selected: $NQ_1 = OP(1:w_s)$. Using the reverse arrangement test, A_{OP} is calculated. The upper and lower limits for A_{PV} and A_{OP} are the same and calculated using **eqs 7** and **8**. While computing μ_A and σ_A , w_s is used in place of M .

Step 5: If $A_{LL}^\alpha < A_{PV} < A_{UL}^\alpha$ (PV is in the steady state in the first data window) and $A_{OP} \notin (A_{LL}^\alpha, A_{UL}^\alpha)$ (OP is in the transient state in the first data window), then $S(1) = 1$, or else $S(1) = 0$. The main difference between the above methods and Method 4 is that in Method 4, the reverse arrangement test is applied to only one data window at a time, whereas the above methods need two consecutive data windows. Steps 3–5 are repeated for the remaining data windows of PV and OP.

Step 6: The stiction index is computed using **eq 6**. If this index is equal to zero, the given control loop experiences oscillations because of a non-stiction condition. Otherwise, the stiction band is approximated using the procedure explained in **Section 3.5**.

3.5. Stiction Quantification. If the given control valve is found behaving abnormally as a result of stiction, it is important to quantify stiction to determine whether the control valve needs immediate replacement (or repair) or panel operators can continue its usage in process operations until a scheduled plant turnaround. The method described in this section makes use of the stiction signal S and OP to estimate the stiction band. **Figure 6** portrays S obtained via one of the proposed methods for CHEM 32 (adopted from ISDB). As explained in **Section 3.1**, during the whole time that the control valve does not move, S stays at the value of one. When the control valve is in motion, S remains at zero. In agreement with **Figure 6**, the control valve is blocked from the first sample through the sixth sample. Therefore, as given in **eq 9**, the absolute difference between the values of OP at the first and sixth samples is the stiction band in that duration.

$$\eta_1 = |OP(1) - OP(6)| \quad (9)$$

At the seventh sample, the control valve recommences varying its position until the 48th sample. It once more becomes sticky at the 49th sample and keeps exhibiting such behavior until the 54th sample. The stiction band within this period is computed as per **eq 10**.

$$\eta_2 = |OP(49) - OP(54)| \quad (10)$$

This way, whenever the control valve is stuck, an approximation for the corresponding stiction band can be attained. The distribution of the estimated stiction bands is depicted in **Figure 7**. The 95th percentile of the set of approximated stiction bands is considered as the overall stiction of the control valve being operated in the control loop CHEM 32.

4. APPLICATION TO INDUSTRIAL CONTROL LOOPS

In this section, the stiction detection capability of the proposed methods is evaluated by applying them to data collected from industrial control loops. The industrial control loops considered embrace twenty control loops from ISDB. The actual malfunction of each of the control loops is known.

4.1. Benchmark Control Loops. The selected benchmark control loops are listed in **Table 1**. For each value of α in the

Table 1. Benchmark Control Loops Taken from ISDB^a

loop name	control loop	actual malfunction
CHEM 1	flow control	stiction
CHEM 2	flow control	stiction
CHEM 3	temperature control	non-stiction
CHEM 6	flow control	stiction
CHEM 10	pressure control	stiction
CHEM 11	flow control	stiction
CHEM 12	flow control	stiction
CHEM 13	analyzer control	non-stiction
CHEM 14	flow control	non-stiction
CHEM 16	pressure control	non-stiction
CHEM 23	flow control	stiction
CHEM 24	flow control	stiction
CHEM 29	flow control	stiction
CHEM 32	flow control	stiction
PAP 2	flow control	stiction
PAP 4	concentration control	non-stiction
PAP 5	concentration control	stiction
PAP 7	flow control	non-stiction
PAP 9	temperature control	non-stiction
MIN 1	temperature control	stiction

^aCHEM—chemicals, PAP—pulp and papers, MIN—mining.

set $\{0.05, 0.025, 0.01\}$, w_s was varied from 3 to 15 with the step size of 1. The results acquired via the proposed methods are displayed in **Figure 8**. **Table 2** provides the optimal values found for w_s and α . For Method 1, four different optimal pairs $((w_s, \alpha) = (3, 0.05), (w_s, \alpha) = (4, 0.05), (w_s, \alpha) = (8, 0.05),$ and $(w_s, \alpha) = (8, 0.025))$ yielded the same number of correct diagnoses. Among those pairs, the third pair was selected. For the remaining methods, unique optimal pairs were obtained.

Using the respective optimal w_s and α , each of the proposed methods was again applied to the twenty benchmark control loops. The control loop: CHEM 2 was chosen to illustrate the working mechanism of the proposed methods. The oscillating PV and OP, which belong to CHEM 2, are depicted in **Figure S1** (given in the Supporting Information). The PV signal occasionally reaches a steady state and remains at this state for some period of time, during which the OP signal constantly changes. This kind of behavior can only be observed in control loops affected by stiction. Results for this control loop are shown in **Figures S2–S13** (given in the Supporting Information). As shown in **Figure S2**, in some data windows, the F-values stay below the critical F-value, which indicates that Method 1 detected steady-state periods in PV. However, the F-values (**Figure S3**) computed for OP are not in agreement with its behavior seen in **Figure S1**. According to **Figure S3**, OP also has several steady states, which is not true. Ideally, most F-values should exceed the critical F-value to identify non-steady-state periods. Because of this, Method 1 could only detect some of the incidences of valve stiction (**Figure S4**). Since noisy PV and OP were considered, the noise hampered the

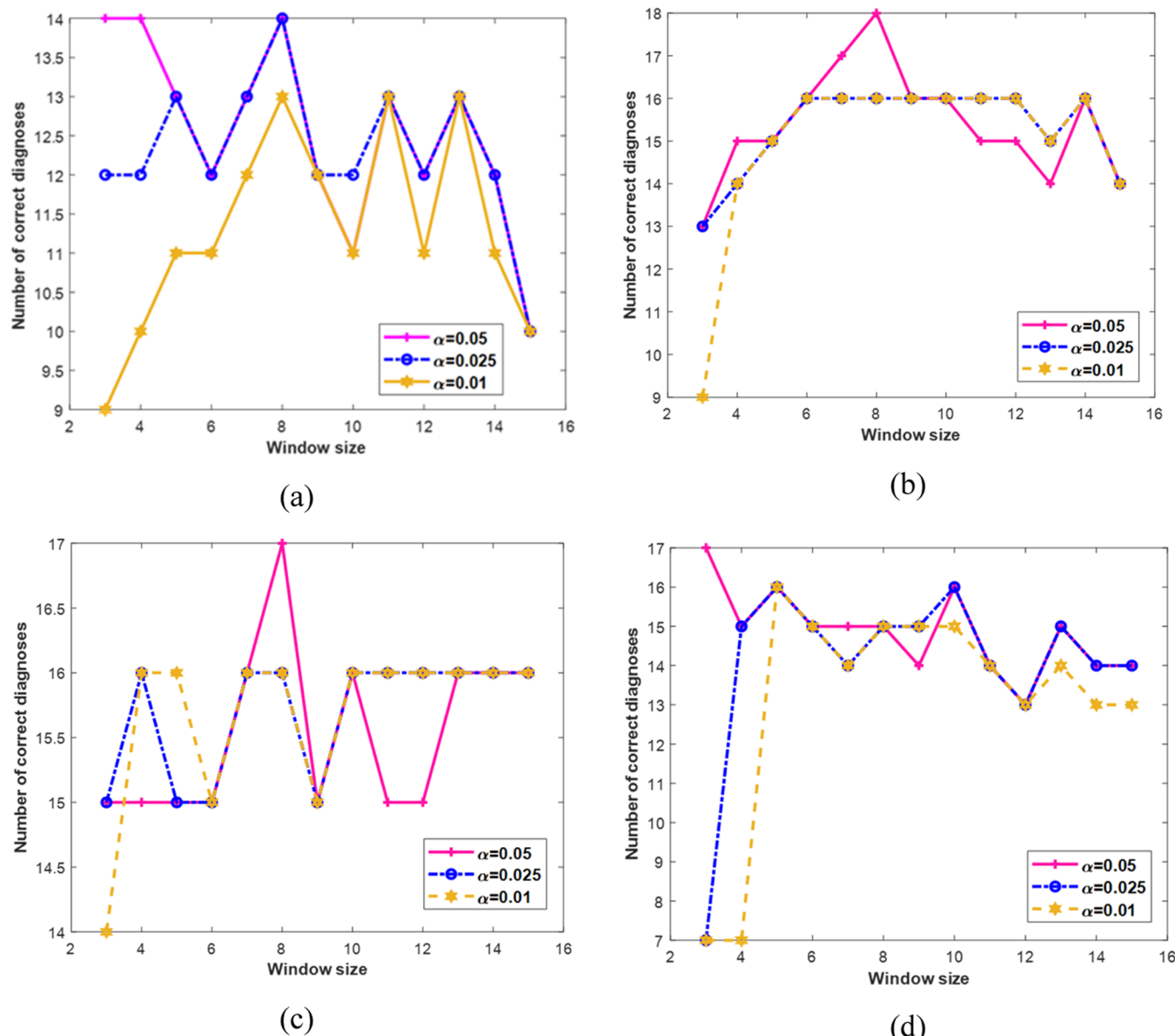


Figure 8. Selection of optimal window size (w_s) and significance level (α). Panel (a) is for Method 1, panel (b) is for Method II, panel (c) is for Method 3, and the last panel is for Method 4.

Table 2. Optimum Values for w_s and α

parameters	method			
	1	2	3	4
w_s	8	8	8	3
α	0.05	0.05	0.05	0.05

stiction detection capability of Method 1. Figures S5 and S6 display the t -test values obtained for PV and OP, respectively. Whenever a steady state is identified in PV, the t_p -value computed using the respective data windows of OP is above the critical t_p -value. Thus, as shown in Figure S7, Method 2 captured all of the data windows in which the control valve is sticky. Similar behavior is noticed from the results (Figures S8–S10) of Method 3. Since the window size of three was determined optimal, Method 4 wrongly treated all of the data windows as incidences of stiction. For the remaining benchmark control loops, results are presented in Tables 3

and 4. The performance of the proposed methods was evaluated using the metrics defined below.

$$\text{accuracy} = \frac{\text{TP} + \text{TN}}{\text{TP} + \text{FP} + \text{TN} + \text{FN}} \quad (11)$$

$$\text{precision} = \frac{\text{TP}}{\text{TP} + \text{FP}} \quad (12)$$

$$\text{recall} = \frac{\text{TP}}{\text{TP} + \text{FN}} \quad (13)$$

$$\text{specificity} = \frac{\text{TN}}{\text{TN} + \text{FP}} \quad (14)$$

$$\text{F}_1 \text{ score} = \frac{2 \times \text{precision} \times \text{recall}}{\text{precision} + \text{recall}} \quad (15)$$

Here, TP is true positive (actual malfunction is stiction, and verdict issued by a proposed method is also stiction), TN is

Table 3. Results for the Benchmark Control Loops

loop name	method 1			method 2		
	Ω	Ψ	diagnosis	Ω	Ψ	diagnosis
CHEM 1	4.9505	0.2410	stiction	8.9109	0.3098	stiction
CHEM 2	8.0645	3.1840	stiction	3.2258	1.6007	stiction
CHEM 3	30.5785	1.5200	stiction	0	0	no-stiction
CHEM 6	9.6774	0.1370	stiction	4.8387	0.0830	stiction
CHEM 10	0	0	no-stiction	19.3548	0.8738	stiction
CHEM 11	4.8387	0.6184	stiction	6.4516	0.4990	stiction
CHEM 12	4.8193	0.1327	stiction	8.8353	0.2849	stiction
CHEM 13	0	0	no-stiction	0	0	no-stiction
CHEM 14	6.4516	2.8244	stiction	24.7312	2.8244	stiction
CHEM 16	16.1290	1.9819	stiction	25.8065	6.6426	stiction
CHEM 23	2.1505	3.6806	stiction	55.9140	24.0139	stiction
CHEM 24	3.2258	22.1902	stiction	2.1505	16.4944	stiction
CHEM 29	7.3415	12.3416	stiction	7.3415	9.1584	stiction
CHEM 32	6.4516	8.1018	stiction	12.9032	12.5687	stiction
PAP 2	13.5135	2.6200	stiction	5.4054	3.2100	stiction
PAP 4	0	0	no-stiction	0	0	no-stiction
PAP 5	7.9146	0.1870	stiction	1.7786	0.2460	stiction
PAP 7	6.3600	0.1750	stiction	0	0	no-stiction
PAP 9	2.6786	0.3126	stiction	0	0	no-stiction
MIN 1	2.4316	0.3197	stiction	4.2553	0.8032	stiction

Table 4. Results for the Benchmark Control Loops

loop name	method 3			method 4		
	Ω	Ψ	diagnosis	Ω	Ψ	diagnosis
CHEM 1	28.7129	0.4588	stiction	23.8889	0.2160	stiction
CHEM 2	14.5161	4.6319	stiction	34.0361	4.3611	stiction
CHEM 3	29.7521	1.3100	stiction	17.9289	1.3700	stiction
CHEM 6	12.9032	0.2220	stiction	16.8675	0.1460	stiction
CHEM 10	38.7097	1.1150	stiction	39.7590	0.4972	stiction
CHEM 11	22.5806	1.0476	stiction	21.3855	0.6645	stiction
CHEM 12	29.7189	0.6667	stiction	33.3835	0.3457	stiction
CHEM 13	0	0	no-stiction	0	0	no-stiction
CHEM 14	33.3333	2.8244	stiction	0	0	no-stiction
CHEM 16	30.1075	6.6426	stiction	29.6593	2.3521	stiction
CHEM 23	78.4946	24.6667	stiction	29.8597	5.9861	stiction
CHEM 24	15.0538	20.0910	stiction	24.0481	14.8865	stiction
CHEM 29	20.0222	9.7721	stiction	9.2122	9.9143	stiction
CHEM 32	26.6129	17.5254	stiction	34.4361	13.5653	stiction
PAP 2	17.5676	3.1600	stiction	17.1285	1.400	stiction
PAP 4	0	0	no stiction	5.5416	0.3940	stiction
PAP 5	5.1578	0.2540	stiction	8.2680	0.1210	stiction
PAP 7	0	0	no-stiction	0	0	no-stiction
PAP 9	0	0	no-stiction	0	0	no-stiction
MIN 1	11.5502	0.8032	stiction	13.9932	0.2501	stiction

true negative (actual malfunction is non-stiction, and verdict issued by a proposed method is also non-stiction), *FP* is false positive (actual malfunction is non-stiction, while verdict issued by a proposed method is stiction) and *FN* is false negative (actual malfunction is stiction, but verdict issued by a proposed method is non-stiction).

Table 5 provides values obtained for the above-mentioned performance metrics. As per Table 6 (full forms for acronyms used in Table 6 are provided in Table S1 in the Supporting Information), the *t*-test-based method (i.e., Method 2 in the present work) demonstrated superior performance over all of the existing methods and Methods 1, 3, and 4 developed in the present work. Both the modified T^2 -test-based method

Table 5. Performance of the Proposed Methods

performance metric	method 1	method 2	method 3	method 4
true positive	12	13	13	13
true negative	2	5	4	4
false positive	5	2	3	3
false negative	1	0	0	0
precision (%)	70.59	86.67	81.25	81.25
recall (%)	92.31	100	100	100
specificity (%)	28.57	71.43	57.14	57.14
F1 score	80	92.86	89.66	89.66
accuracy	70	90	85	85

Table 6. Comparison with Existing Methods^a

SDM	NCD	SDM	NCD	SDM	NCD
MD1	14	CNN-PCA	16	RELAY ²⁶	13
MD2	18	BIC ²²	16	ZONE ²⁷	13
MD3	17	SDN ²³	15	GLCM-NN	12
MD4	17	HAMM2 ⁴	15	CURVE ²⁸	12
SF ¹⁹	17	HAMM3 ⁴	14	SLOPE ²⁷	12
LR ²⁰	17	LBP-NN	13	NLPCA-AC ²⁹	11
BSD ²¹	17	CORR ²⁴	13	AREA ³⁰	10
KMW ⁵	16	HIST ²⁵	13		

^aSDM—stiction detection method, NCD—number of correct diagnoses, MD1 to MD4 are proposed methods.

(Method 3) and reverse arrangement test-based method (Method 4) showed similar performance as SF, LR, and BSD and outpaced the rest of the existing methods. However, the *F*-test-based method (Method 1) failed to issue a correct verdict in six of the twenty benchmark control loops.

4.2. Testing Proposed Methods under Various Scenarios. 4.2.1. *Good Control Loop.* Figure S14 (given in the Supporting Information) displays the block diagram of the concentration control loop. Equations 16 and 17 provide the process model and the controller transfer function considered in the control loop. Data-based valve stiction model proposed by Shoukat Choudhury et al.¹⁸ was adopted.

$$G_p = \frac{3e^{-10s}}{10s + 1} \quad (16)$$

$$G_c = 0.2 \left(\frac{10s + 1}{10s} \right) \quad (17)$$

The following three cases are considered to determine whether or not the proposed methods detect stiction, even if the control loop performs satisfactorily.

Case 1: The control loop performs well, i.e., perfectly tracks the setpoint. There is no effect of noise or disturbance (servo problem).

Case 2: The process is disturbed by the input disturbance (regulatory problem).

Case 3: The process output (PV) is corrupted with noise (servo problem with noisy PV).

In all of the three cases, the control valve is healthy and does not suffer from any kind of fault; hence, the control valve position is exactly equal to OP. For each of the three cases, simulation was run for 800 s. Figures S15–S17 display the closed-loop signals for Cases 1, 2, and 3, respectively. The closed-loop signals obtained from each case were analyzed by the proposed methods. Table S2 (given in the Supporting Information) provides the results obtained from the proposed methods. Method 1 did not detect stiction in Cases 1 and 3. For Case 2, the estimated stiction band is negligible; hence, the diagnosis indicated no stiction. The results acquired from Methods 2, 3, and 4 are in agreement with the nonsticky condition of the valve. Based on Figures S15–S17 and Table S2, the following inferences were drawn.

- Since the control valve is not sticky and the control loop is not affected by any non-stiction condition, there are no oscillations in PV and OP.
- In the case of servo problem, initially, both PV and OP changed and then settled at their respective steady states. When PV was varying, OP also experienced variations. When PV stayed in its new steady state, OP also

remained in its steady state. Therefore, the proposed methods did not detect stiction.

- When the process was affected by the disturbance, PV deviated from SP. So the controller modified OP to bring PV back to SP. The moment the controller was able to maintain PV at SP, OP also reached a steady state. In this case too, both PV and OP remained in either the transient phase or the steady-state phase. This is the reason that the proposed methods did not find stiction.
- As noticed from the results attained for the benchmark control loops, the proposed methods possess a certain degree of robustness to noise in PV and OP. Hence, the noise could not significantly hamper the performance of the methods.
- In all of the three situations explained above, the signature behavior of a control loop suffering from stiction (shown in Figure 2) was not found; hence, the proposed methods yielded the correct verdict.

4.2.2. Simultaneous Occurrence of Stiction and Disturbances. At times, control loops may be affected by both stiction and non-stiction conditions (for instance, disturbances). When the control valve is sticky, disturbances may enter the process. When this happens, PV and OP oscillate as a result of both conditions occurring at the same. To simulate this situation, the concentration control loop shown in Figure S14 was considered. The same process model and the controller transfer function were used. For the valve stiction model, stiction band (*S*) of 15 and slip-jump (*J*) of 5 were employed. Figure S18 (given in the Supporting Information) depicts PV and OP. A unit step change was made in SP at time 0. A unit step change was introduced in the disturbance variable at time 50 s. Even though both stiction and disturbances affected the control loop, PV still intermittently reached a steady state because of valve stiction. As per Table S3 (given in the Supporting Information), the proposed methods successfully detected the presence of stiction.

4.2.3. Stiction Detection in Cascade Control Loop. The cascade control loop (shown in Figure S19 in the Supporting Information) is considered to check if the proposed methods detect stiction in cascade control loops. The following equations provide the transfer function models adopted for the cascade loop.

$$G_{p1} = \frac{10}{(s + 1)^3} \quad (18)$$

$$G_{p2} = \frac{3}{s + 2} \quad (19)$$

$$G_{c1} = 0.015 \left(1 + \frac{1}{0.716 s} \right) \quad (20)$$

$$G_{c2} = 0.244 \left(1 + \frac{1}{0.134 s} \right) \quad (21)$$

In the cascade control loop, the master controller (controller in the outer control loop), based on measured PV1, generates OP1 that is setpoint to the slave controller (controller in the inner control loop). Based on the setpoint received, the slave controller alters its output (OP2) to adjust the valve position of the control valve. Only the inner control loop has the control valve. If there is stiction in the control valve, it can be detected using OP2 and PV2 (or PV1). The same valve

stiction model used in Sections 4.2.1 and 4.2.2 was utilized in this section to create stiction in the cascade control loop. The following parameters were considered for the valve stiction model.

$$S = 15, J = 2 \quad (22)$$

The control loop was operated for 3000 s. The closed-loop signals of the outer and inner loops are depicted in Figures S20 and S21 (Supporting Information). The proposed methods were applied to the closed-loop signals of the inner loop, and the results are bestowed in Table S3. It can be noticed that the proposed methods detected stiction.

4.3. Pros and Cons of the Proposed Methods. Merits and demerits of the proposed methods are listed in Table 7. If

Table 7. Characteristics of the Proposed Methods

criterion	MD1	MD2	MD3	MD4
requires routine operation data	yes	yes	yes	yes
practically implementable	yes	yes	yes	yes
applicable to all control loops except level loop	yes	yes	yes	yes
quick stiction detection	yes	yes	yes	yes
capable of quantifying stiction	yes	yes	yes	yes
valid for control loops with constant or varying setpoint	yes	yes	yes	yes
depends on waveform or limit cycles	no	no	no	no
applicable to loops with multiple oscillations	yes	Yes	yes	yes
robustness to noise in PV and OP	no	Yes	yes	yes
involves extensive training	no	No	no	no
entails complex computations	no	No	yes	no
exhibits comparable or better performance than the existing methods	no	Yes	yes	yes

the answer is in blue (bold text) for any of the criteria listed in the first column of the table, then it is a desirable property (or advantage). Otherwise (italic text), it is of a disadvantage. From the results of Sections 4.1 and 4.2 and Table 7, it can be noticed that while each proposed method has its pros and cons and can be applied to different scenarios, Method 2 appears to have accomplished an overall balance between complexity and effectiveness.

5. CONCLUSIONS

Control loops with sticky valves often contribute to production loss and reduced profits. It is important to identify sticky control valves in a timely manner. In the present work, four data-driven stiction detection and quantification methods were developed to diagnose oscillating control loops. The proposed methods can be applied to all types of control loops except level loops. The first three methods demonstrated a satisfactory performance in the benchmark control loops. The last method is sensitive to noise in the closed-loop signals of the control loops, which makes it less effective in identifying sticky control valves. On the contrary, the first three methods are impervious to noisy PV and OP; hence, they can work well in industrial settings where noise is inevitable.

■ ASSOCIATED CONTENT

SI Supporting Information

The Supporting Information is available free of charge at <https://pubs.acs.org/doi/10.1021/acs.iecr.2c03564>.

Results obtained for CHEM 2 via the proposed methods, full forms for acronyms used in Table 6, and results for Section 4.2 (PDF)

■ AUTHOR INFORMATION

Corresponding Author

Biao Huang – Department of Chemical and Materials Engineering, University of Alberta, Edmonton T6G 2G6 Alberta, Canada; orcid.org/0000-0001-9082-2216; Email: bhuang@ualberta.ca

Authors

Seshu K. Damarla – Department of Chemical and Materials Engineering, University of Alberta, Edmonton T6G 2G6 Alberta, Canada; orcid.org/0000-0002-3875-0697

Xi Sun – Syncrude Canada Limited, Fort McMurray, Alberta, Canada T9H 3L1

Fangwei Xu – Syncrude Canada Limited, Fort McMurray, Alberta, Canada T9H 3L1

Ashish Shah – Syncrude Canada Limited, Fort McMurray, Alberta, Canada T9H 3L1

Complete contact information is available at:

<https://pubs.acs.org/10.1021/acs.iecr.2c03564>

Notes

The authors declare no competing financial interest.

■ REFERENCES

- (1) Ding, S. X.; Li, L. Control performance monitoring and degradation recovery in automatic control systems: A review, some new results, and future perspectives. *Control Eng. Pract.* **2021**, *111*, No. 104790K.
- (2) Huang, B.; Shah, S. L. *Performance Assessment of Control Loops: Theory and Applications*; Springer-Verlag: London, 1999; pp 1–275.
- (3) Bialkowski, W. L. Dreams Versus Reality: A View from Both Sides of the Gap. *Pulp Pap. Can.* **1993**, *94*, 19–27.
- (4) Jelali, M.; Huang, B. *Detection and Diagnosis of Stiction in Control Loops: State of the Art and Advanced Methods*; Springer-Verlag: London, 2009; pp 1–389.
- (5) Zheng, D.; Sun, X.; Damarla, S. K.; Shah, A.; Amalraj, J.; Huang, B. Valve Stiction Detection and Quantification Using a K-Means Clustering Based Moving Window Approach. *Ind. Eng. Chem. Res.* **2021**, *60*, 2563–2577.
- (6) Bacci di Capaci, R.; Scali, C. Review and Comparison of Techniques of Analysis of Valve Stiction: From Modeling to Smart Diagnosis. *Chem. Eng. Res. Des.* **2018**, *130*, 230–265.
- (7) Kok, T. L.; Aldrich, C.; Zabiri, H.; Ammar, S. A.; Olivier, J. Application of unthresholded recurrence plots and texture analysis for industrial loops with faulty valves. *Soft Comput.* **2022**, *26*, 10477–10492.
- (8) Arbabi Yazdi, Y.; Shandiz, H. T.; Narm, H. G. Stiction detection in control valves using a support vector machine with a generalized statistical variable. *ISA Trans.* **2022**, *126*, 407–414.
- (9) Henry, Y. Y. S.; Aldrich, C.; Zabiri, H. Detection and Severity Identification of Control Valve Stiction in Industrial Loops using Integrated Partially Retrained CNN-PCA Frameworks. *Chemom. Intell. Lab. Syst.* **2020**, *206*, No. 104143.
- (10) Zhang, K.; Liu, Y.; Gu, Y.; Ruan, G. X.; Ruan, X.; Wang, J. Multiple Timescale Feature Learning Strategy for Valve Stiction Detection Based on Convolutional Neural Network. *IEEE/ASME Trans. Mechatron.* **2022**, *27*, 1478–1488.
- (11) Schiefer, H.; Schiefer, F. *Statistics for Engineers: An Introduction with Examples from Practice*; Springer Nature: Germany, 2021; pp 1–130.
- (12) Ying, Y. An Approximate Degrees-of-Freedom Solution to the Multivariate Behrens-Fisher Problem. *Biometrika* **1965**, *52*, 139.

- (13) Narasimhan, S.; Mah, R. S. H.; Tamhane, A. C.; Woodward, J. W.; Hale, J. C. A composite statistical test for detecting changes of steady states. *AIChE J.* **1986**, *32*, 1409–1418.
- (14) Huang, T. Steady State and TransientState Identification in an IndustrialProcess. MSc Thesis; Oklahoma State University: USA, 2013.
- (15) Bendat, J. S.; Piersol, A. G. *Random Data: Analysis and Measurement Procedures*; Wiley: USA, 2010; pp 1–467.
- (16) Huang, B-L.; Yao, Y. Automatic steady state identification for batch processes by nonparametric signal decomposition and statistical hypothesis test. *Chemom. Intell. Lab. Syst.* **2014**, *138*, 84–96.
- (17) Kelly, J. D.; Hedengren, J. D. A steady-state detection (SSD) algorithm to detect non-stationary drifts in processes. *J. Process Control* **2013**, *23*, 326–331.
- (18) Shoukat Choudhury, M. A. A.; Thornhill, N. F.; Shah, S. L. Modelling Valve Stiction. *Control Eng. Pract.* **2005**, *13*, 641–658.
- (19) Damarla, S. K.; Sun, X.; Xu, F.; Shah, A.; Huang, B. *A Sigmoid Function based Method for Detection of Stiction in Control Valves*, Proceedings of 7th International Symposium on Advanced Control of Industrial Processes, Vancouver, 2022; pp 210–215.
- (20) Damarla, S. K.; Sun, X.; Xu, F.; Shah, A.; Amalraj, J.; Huang, B. Practical Linear Regression-Based Method for Detection and Quantification of Stiction in Control Valves. *Ind. Eng. Chem. Res.* **2022**, *61*, 502–514.
- (21) Kamaruddin, B.; Zabiri, H.; Mohd Amiruddin, A. A. A.; Teh, W. K.; Ramasamy, M.; Jeremiah, S. S. A Simple Model-Free Butterfly Shape-Based Detection (BSD) Method Integrated with Deep Learning CNN for Valve Stiction Detection and Quantification. *J. Process Control* **2020**, *87*, 1–16.
- (22) Choudhury, M. A. A. S.; Shook, D. S.; Shah, S. L. Linear or Nonlinear? A Bicoherence Based Metric of Nonlinearity Measure. *IFAC Proc. Vol.* **2006**, *39*, 617–622.
- (23) Mohd Amiruddin, A. A. A.; Zabiri, H.; Jeremiah, S. S.; Teh, W. K.; Kamaruddin, B. Valve Stiction Detection Through Improved Pattern Recognition Using Neural Networks. *Control Eng. Pract.* **2019**, *90*, 63–84.
- (24) Horch, A. A Simple Method for Detection of Stiction in Control Valves. *Control Eng. Pract.* **1999**, *7*, 1221–1231.
- (25) Horch, A.; Isaksson, A. J. In *Detection of Valve Stiction in Integrating Processes*, Proceedings of the European Control Conference, Porto, 2001; pp 1327–1332.
- (26) Rossi, M.; Scali, C. Automatic Detection of Stiction in Actuators: A Technique to Reduce the Number of Uncertain Cases. *IFAC Proc. Vol.* **2004**, *37*, 751–756.
- (27) Dambros, J. W. V.; Farenzena, M.; Trierweiler, J. O. Data-Based Method to Diagnose Valve Stiction with Variable Reference Signal. *Ind. Eng. Chem. Res.* **2016**, *55*, 10316–10327.
- (28) He, Q. P.; Wang, J.; Pottmann, M.; Qin, S. J. A Curve Fitting Method for Detecting Valve Stiction in Oscillating Control Loops. *Ind. Eng. Chem. Res.* **2007**, *46*, 4549–4560.
- (29) Teh, W. K.; Zabiri, H.; Samyudia, Y.; Jeremiah, S. S.; Kamaruddin, B.; Mohd Amiruddin, A. A. A.; Ramli, N. M. An Improved Diagnostic Tool for Control Valve Stiction Based on Nonlinear Principle Component Analysis. *Ind. Eng. Chem. Res.* **2018**, *57*, 11350–11365.
- (30) Singhal, A.; Salsbury, T. I. A Simple Method for Detecting Valve Stiction in Oscillating Control Loops. *J. Process Control* **2005**, *15*, 371–382.

□ Recommended by ACS

Computational Investigation of the Role of Eccentricity and Wall Wettability on Liquid Draining from a Storage Tank

Ranjana Rathaur and Sumana Ghosh

APRIL 04, 2023

INDUSTRIAL & ENGINEERING CHEMISTRY RESEARCH

READ ↗

Novel Liquid Distributor Concept for Rotating Packed Beds

Tobias Pyka, Gerhard Schembecker, et al.

MARCH 28, 2023

INDUSTRIAL & ENGINEERING CHEMISTRY RESEARCH

READ ↗

Semiempirical Model of the Drag Force Acting on an Obstacle in Downward Dense Particle Flows as per the Flow-Around Behavior

Xiandong Liu, Yang Zhang, et al.

JANUARY 30, 2023

INDUSTRIAL & ENGINEERING CHEMISTRY RESEARCH

READ ↗

Control of the Multi-Timescale Process Using Multiple Timescale Recurrent Neural Network-Based Model Predictive Control

Ngiam Li Jian, Marappagounder Ramasamy, et al.

APRIL 10, 2023

INDUSTRIAL & ENGINEERING CHEMISTRY RESEARCH

READ ↗

Get More Suggestions >